

Electronic Supplementary Information for

***In vitro* anticancer evaluation of Enceleamycin A and its underlying
mechanism**

Abujunaid Khan^{ab}, S. Pradeep^{ab} and Syed G Dastager^{*ab}

^a NCIM-Resource Center, Biochemical Sciences Division, CSIR-National Chemical Laboratory, Pune-411008, India;

^b Academy of Scientific and Innovative Research (AcSIR), Ghaziabad – 201002, India

*Corresponding E-mail : sg.dastager@ncl.res.in

Sr. No.	Table of Contents	Page no.
1.	Purification and analysis of Enceleamycins	3-6
2.	Anticancer activity of Enceleamycins	7-11
3.	Molecular docking of Enceleamycin A	12-13
4.	MD Simulation of docked complex Enceleamycin A and AKT2	14
5.	<i>In silico</i> ADMET study for Enceleamycin A, B and C	15-18
	Reference	19

1. Purification and analysis of Enceleamycins

The compounds were isolated from rare Actinobacteria, *Amycolatopsis* sp. MCC 0218. The fermentation was carried out in static condition and crude extract yielded after ethyl acetate extraction was further purified using silica gel column chromatography followed by semi-preparative HPLC. The details of the purification and structural elucidation can be obtained from our previous article.¹

HPLC: The three furo-naphthoquinones named as Enceleamycin A-C and the purified compounds were analysed by analytical U-HPLC Thermo Scientific Ultimate 3000 equipped with a VWD detector using reverse phase C-18 Hypersil GOLD (4.6 × 250 mm, 5 µm particle size, thermoscientific, USA) column with the gradient mobile phase of Milli Q Water and Acetonitrile (ACN). The gradient starts from 5% ACN upto 4 minutes and then it increases upto 95% at 17 minutes and maintained at 95% upto 18 min followed by decrease of ACN to 5% at 21 minute and further maintained at 5% upto 25 minute run with a flow rate of 1 ml/min.

HR-ESIMS: HR-ESIMS analysis was carried out on an Agilent 6530 Accurate-Mass Quadrupole Time-of-Flight (Q-TOF) (Agilent, USA) mass spectrometer connected to an HPLC Prime Infinity II 1260 system (800 bar), and a dual electrospray ionization (ESI) source was used for ionization. For LC-based metabolite separation, a Hypersil GOLD C₁₈ (2.1 × 150 mm, 1.9 µm particle size, Thermo Scientific, USA) column was used at 40 °C with a flow rate of 0.3 mL/min. The metabolites were separated using a 20 min gradient with 100% MS grade water (Solvent A) and 100% MS grade acetonitrile (Solvent B) both containing 0.1% formic acid. The LC method started with 2% B for the first 0.3 min and increased to 30% in the next 2 min. The B% was increased from 30% to 45% till 7 min and further increased to 98% to 16 min at which it was held for the next 1 min. The column was equilibrated to the initial ratio of solvents (98% A: 2% B) in the last 3 min. The MS data was acquired in 2 GHz extended dynamic range. The MS parameters are tuned as; gas temperature 325°C, drying gas 10 L/min, and nebulizer at 35 psi and fragmentor 120 volts.

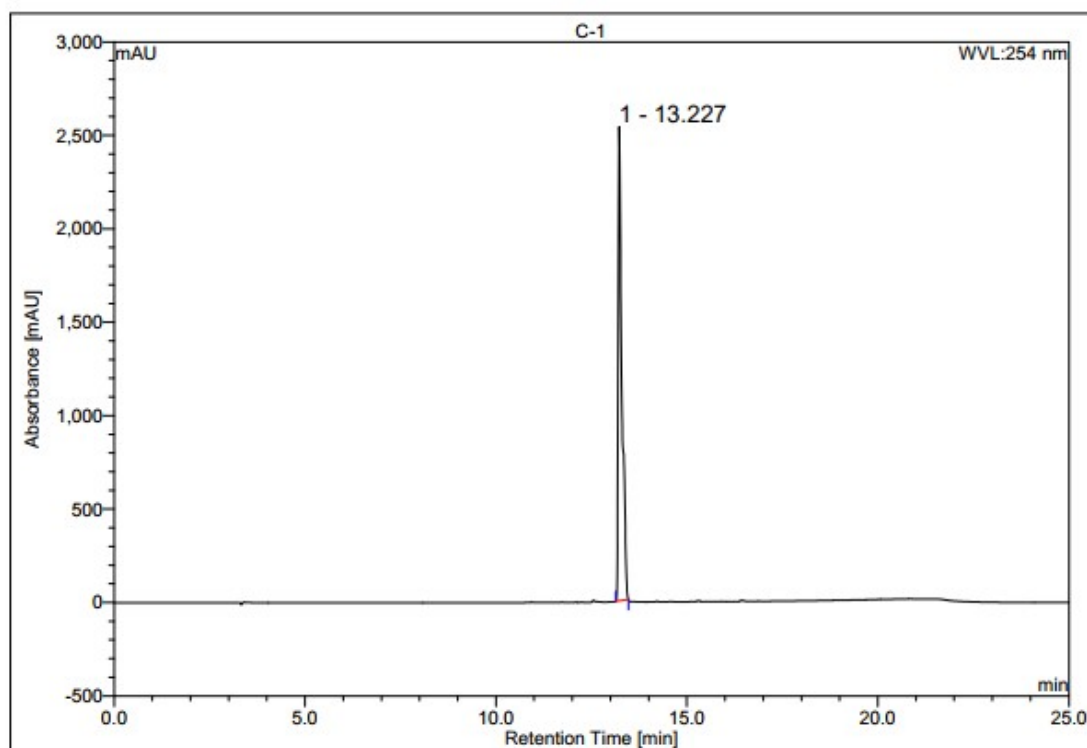


Fig. S1 HPLC chromatogram of Enceleamycin A (C-1)

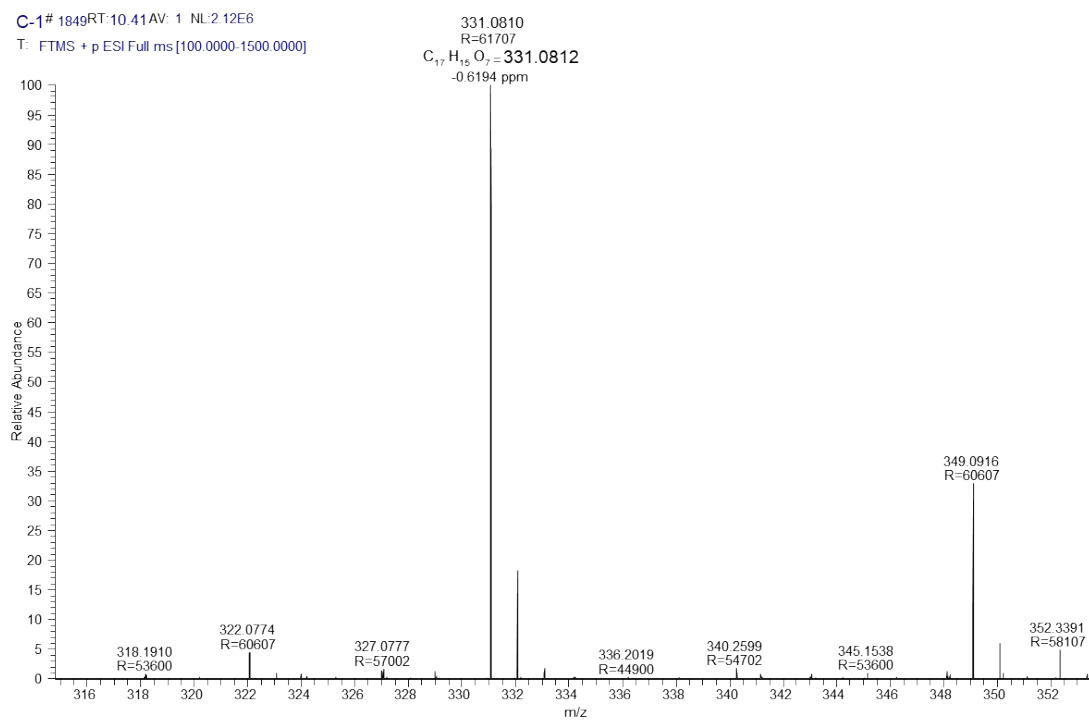


Fig. S2 HR-ESIMS of Enceleamycin A (C-1)

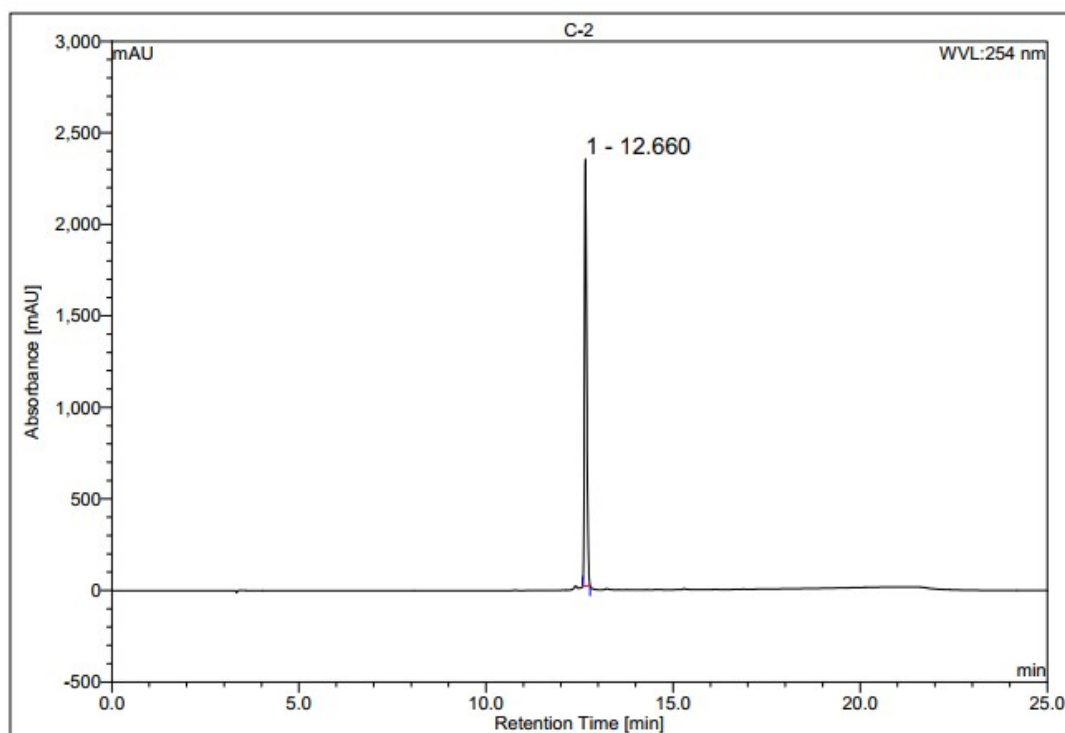


Fig. S3 HPLC chromatogram of Enceleamycin B (C-2)

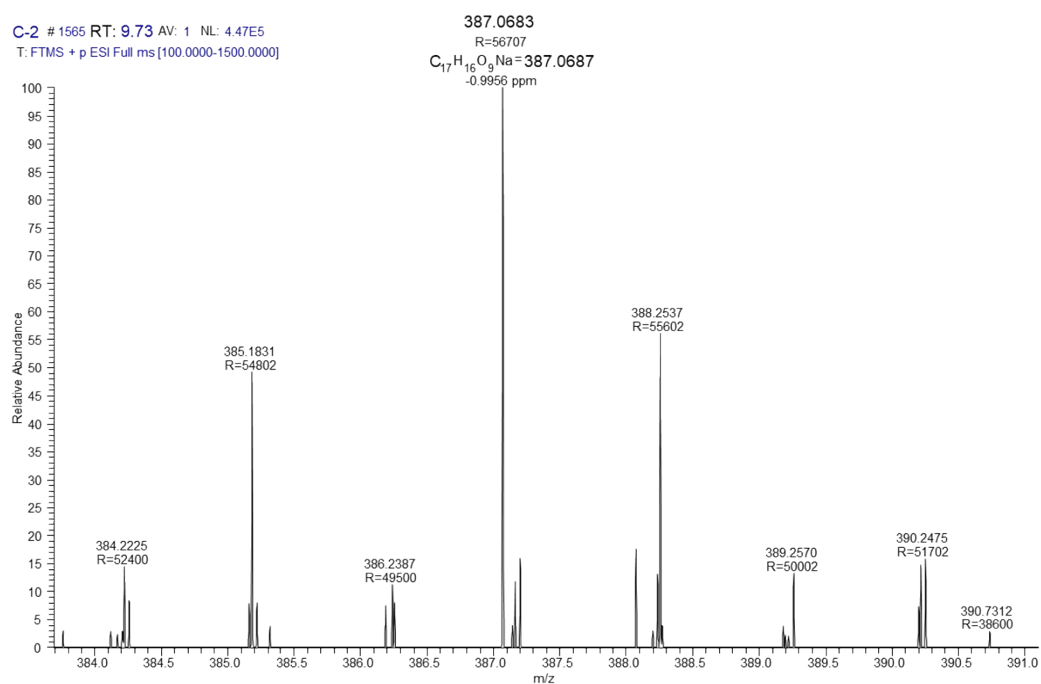


Fig. S4 HR-ESIMS of Enceleamycin B (C-2)

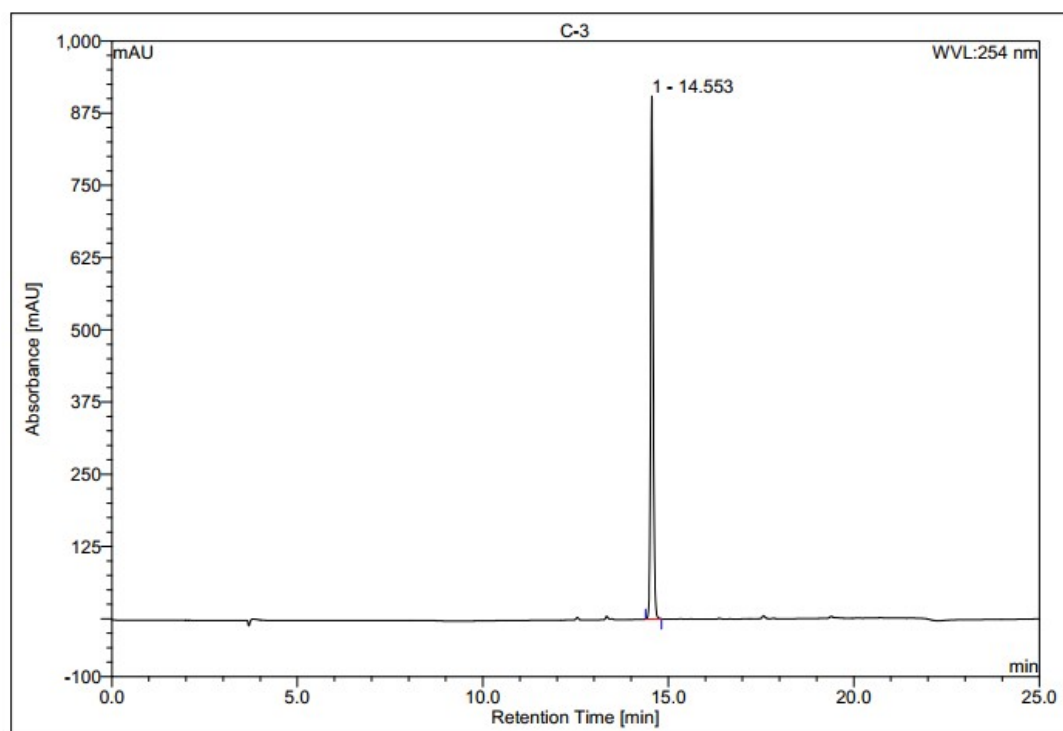


Fig. S5 HPLC chromatogram of Enceleamycin C (C-3)

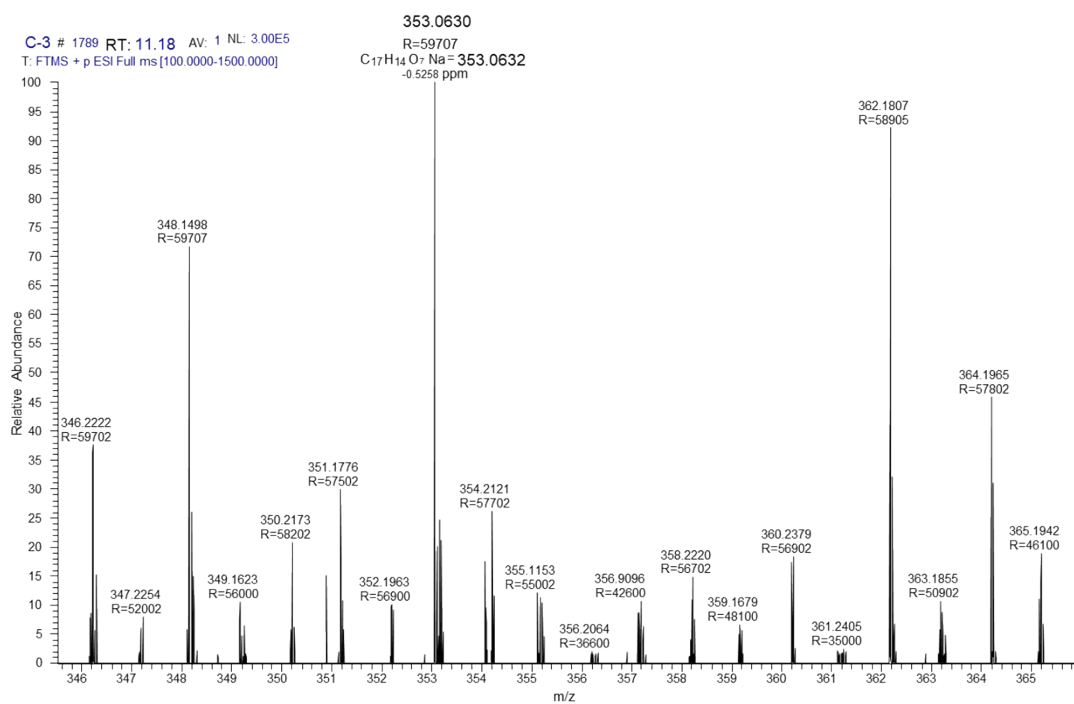


Fig. S6 HR-ESIMS of Enceleamycin C (C-3)

2. Anticancer activity of Enceleamycins

Procedure for Sulforhodamine B (SRB) assay

The cell lines were grown in an appropriate medium containing 10% FBS and 2 mM L-glutamine. For the present screening experiment, 5000 cells/well were inoculated into 96-well microtiter plates. The microtiter plates were incubated at 37° C, 5 % CO₂, for 24 h before adding experimental drugs.

Experimental drugs were solubilized in an appropriate solvent at 100mg/ml, diluted to 1mg/ml using water, and stored frozen before use. At the time of drug addition, an aliquot of frozen concentrate (1mg/ml) was thawed and diluted to 100 µg/ml with a complete medium containing the test article. Aliquots of 10 µl of these different drug dilutions were added to the appropriate microtiter wells already containing 90 µl of medium, resulting in the required final drug concentrations, i.e..10 µg/ml.

After compound addition, the plates were incubated at standard conditions for 48 hours, and the addition of cold TCA terminated the assay. Cells were fixed *in situ* by gently adding 50 µl of cold 30 % (w/v) TCA (final concentration, 10 % TCA) and incubated for 60 minutes at 4°C. The supernatant was discarded; the plates were washed five times with tap water and air-dried. Sulforhodamine B (SRB) solution (50 µl) at 0.4 % (w/v) in 1 % acetic acid was added to each of the wells, and plates were incubated for 20 minutes at room temperature. After staining, the unbound dye was recovered, and the residual dye was removed by washing five times with 1 % acetic acid. The plates were air-dried. The bound stain was subsequently eluted with 10 mM trizma base, and the absorbance was read on a plate reader at 540 nm with a 690 nm reference wavelength.^{1,2}

Percent growth was calculated plate-by-plate for test wells relative to control wells. Percent Growth (GP) was expressed as the ratio of the average absorbance of the test well to the average absorbance of the control wells * 100.

Result of Sulforhodamine B (SRB) assay

From the three novel furo-naphthoquinones, Enceleamycin A was isolated in reasonable quantity and used for the *in vitro* anticancer activity by the Anticancer Drug screening facility (ACDSF) at ACTREC, Tata Memorial Centre, Navi Mumbai, India. The anticancer activity was performed by the Sulforhodamine B (SRB) assay at one dose of 10 µg/ml (30.27µM) against nine human cancer cell lines originating from breast, liver, colon, oral, cervical, lung, prostate, ovarian, and leukemia. The data analysis (Table S1) was based on growth percent (GP), where a lower GP value displays a higher growth inhibition percentage (GI%) calculated as (GI% =100-GP). The GP value negative corresponds to lethal activity, whereas the increased negative value corresponds to the higher activity of the tested compound. Enceleamycin A displayed lethal activity against all the cancer cell lines tested and showed maximum cytotoxicity towards the breast cancer cells with a GP value of -90.6, followed by lung cancer. The compound showed better activity than the anticancer drug Adriamycin against most cancer cell lines.

Table S1. The percentage growth inhibition (%GI) or lethality of Enceleamycin A and Adriamycin against cancer cell line at 10 µg/ml (30.27µM)

Human cancer type	Cell line name	Enceleamycin A	Adriamycin
Breast	MCF-7	-90.6	-81.3
Liver	Hep-G2	-64.6	-39.1
Colon	HT-29	-32.0	97.1 a
Oral	SCC-40	-32.5	-73.7
Cervical	SiHa	-31.2	-59.4
Lung	Hop-62	-85.5	98.9 a
Prostate	PC-3	-76.4	-25.3
Ovarian	SK-OV-3	-78.7	-25.5
Leukemia	HL-60	-36.7	-9.3

^a Percentage growth inhibition (%GI) = 100 - GP (Growth percentage). ^b Negative values correspond to the lethality of the respective cancer cell line.

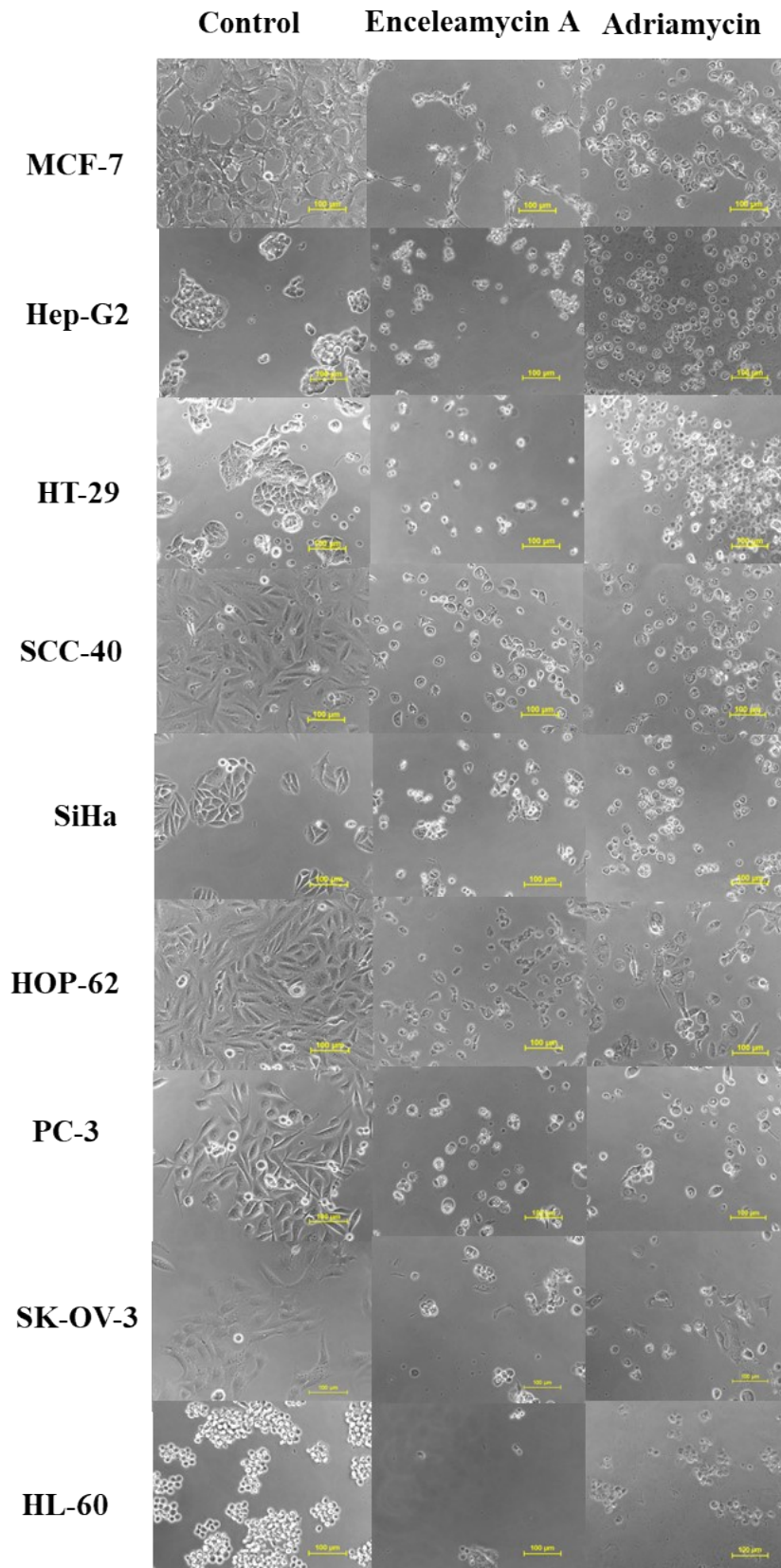


Fig. S7 Morphological change in various cell lines after treatment with Enceleamycin A and adriamycin at 10 $\mu\text{g/ml}$.

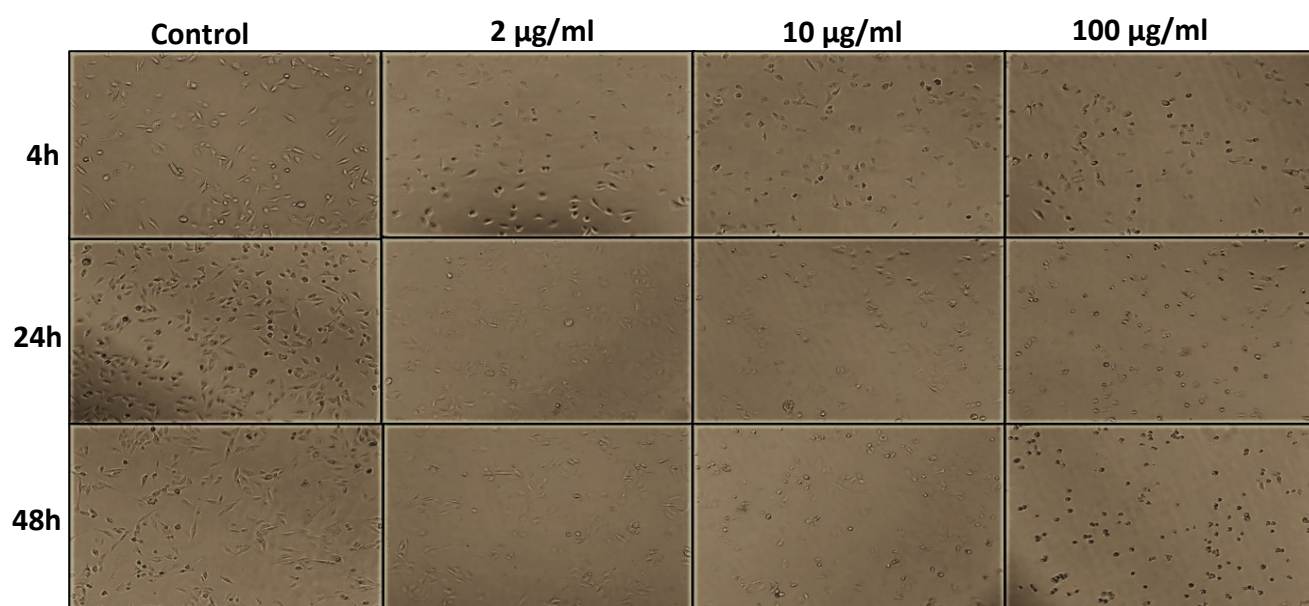


Fig. S9 Effect of Enceleamycin A on the morphology of MDA-MB-231 cells after treatment at 4h, 24h and 48h

2. Molecular docking of Enceleamycin A

Running AutoGrid and AutoDock

The AutoGrid was executed by providing the AutoGrid executable and GPF files as input and converted to the grid log file (GLG) as the output file. After the successful execution of AutoGrid, the genetic algorithm was set to default and is as follows: i) the number of GA runs 10; ii) population size: 150; iii) the number of energy evaluations: 2.5 million (2.0 Å clustered tolerance) and iv) the number of generations 27000. The Lamarckian genetic algorithm was used, and the output was saved in the docking parameter file (DPF) format. The AutoDock was executed by providing the AutoDock executable and DPF files as input, converted to the docking log file (DLG), and docking was launched. The final DLG file contained essential details, the top ten free binding energy energies for every run, and the inhibitory constant. The results were analyzed and ranked based on their binding energies, saved in PDBQT format; the lowest binding energy complex was saved in PDB format for further analysis.

Table S3. Molecular docking of Enceleamycin A with different proteins associated with PI3K-AKT-mTOR pathway

Receptor PDB ID	Receptor Name	Binding affinity (Kcal/mol)
4TV3	PI3K α	-6.87
3O96	AKT1	-6.58
1O6L	AKT2	-7.14
1E7U	mTOR	-6.65
3A62	S6K1	-6.34

Binding Energy = - 7.14 Kcal/mol

Ligand Efficiency = - 0.3

Inhibitory constant = 5830nM

Intermolar energy = - 7.74 Kcal/mol

Vander Waal and desolvation energy = - 7.32 Kcal/mol

Electrostatic energy = - 0.42 Kcal/mol

Total internal energy = 0.46 Kcal/mol

Torsional energy = 0.6 Kcal/mol

Fig. S10 Conformation of the best molecular fit of Enceleamycin A and AKT2 (PDB ID1O6L)

Table S4. RMSD table of Enceleamycin A and the protein AKT2, PDB ID 1O6L

Cluster Rank	Binding Energy (Kcal/mol)	Cluster RMSD (Å)	Reference RMSD (Å)
1	-7.14	0	105.39
2	-7.13	0.1	105.39
3	-7.13	0.09	105.4
4	-6.59	0	127.31
5	-6.26	0	111.82
6	-6.22	0	107.57
7	-5.57	0	108.9
8	-5.42	0	138.79
9	-5.37	0.22	138.76
10	-5.34	0	126.22

Table S5. Non-bond interactions between AKT2 protein and Enceleamycin A (EA)

Name	Distance (Å)	Category	Types	From (Donor)	To (Acceptor)
LYS A: 181: HZ1 - EA: O	2.20784	Hydrogen Bond	Conventional Hydrogen Bond	LYS A:181: HZ1	EA: O
EA: H - GLU A: 200: OE1	2.04415	Hydrogen Bond	Conventional Hydrogen Bond	EA: H	GLU A: 200: OE1
EA: C – GLY A: 295: O	3.41985	Hydrogen Bond	Carbon Hydrogen Bond	EA: C	GLY A: 295: O
EA: C – ASP A: 293: OD1	3.69348	Hydrogen Bond	Carbon Hydrogen Bond	EA: C	ASP A: 293: OD1
GLU A: 193: OE1 - EA	4.00257	Electrostatic	Pi-Anion	GLU A: 193: OE1	EA
PHE A: 163 - EA	3.61776	Hydrophobic	Pi-Pi Stacked	PHE A: 163	EA
EA:C – LEU A: 183	4.55503	Hydrophobic	Alkyl	EA: C	LEU A: 183
EA – LYS A: 191	5.27434	Hydrophobic	Pi-Alkyl	EA	LYS A: 191

3. MD Simulation of docked complex Enceleamycin A and AKT2

Table S6. MM-PBSA assessment giving the free energy calculations from the MD simulation.

Energy summary	Values (Kcal/mol)
van der Waal energy	-32.672 \pm 3.159
Electrostatic energy	-24.456 \pm 2.752
Polar solvation energy	50.566 \pm 3.774
SASA energy	-3.919 \pm 0.252
SAV energy	0.00
WCA energy	0.00
Binding energy	-10.481 \pm 3.398

4. *In silico* ADMET study for Enceleamycin A, B and C

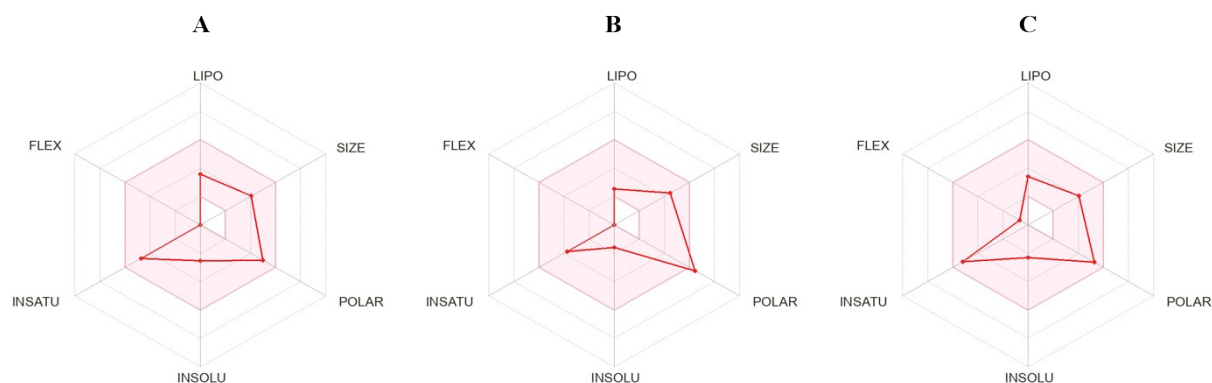


Fig. S11 Bioavailability radar of Enceleamycin A, B and C by SwissADME. Enceleamycin A and C follow the recommended physicochemical properties for bioavailability in all the aspects whereas Enceleamycin B overrules only the polarity criteria.

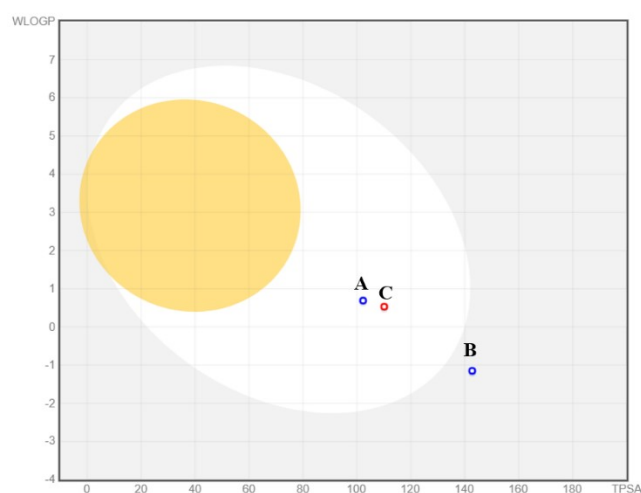


Fig. S12 Boiled egg ADME prediction of Enceleamycin A, B and C by SwissADME. Enceleamycin A and C displaying good GI-absorption whereas Enceleamycin B possess low GI-absorption. All the three molecules are non-permeable to BBB. Enceleamycin B displaying slightly higher TPSA value than recommended.

Table S7. Physicochemical properties of Enceleamycins A-C by SwissADME

Physicochemical properties	Enceleamycin A	Enceleamycin B	Enceleamycin C
Formula	C ₁₇ H ₁₄ O ₇	C ₁₇ H ₁₆ O ₉	C ₁₇ H ₁₄ O ₇
Molecular weight	330.29 g/mol	364.30 g/mol	330.29 g/mol
Number heavy atoms	24	26	24
Number aromatic heavy atoms	6	6	6
Fraction Csp3	0.41	0.53	0.35
Number of rotatable bonds	0	0	1
Number H-bond acceptors	7	9	7
Number H-bond donors	2	4	2
Molar Refractivity	78.07	80.94	79.29
TPSA	102.29 Å ²	142.75 Å ²	110.13 Å ²

Table S8. Lipophilicity properties of Enceleamycins A-C by SwissADME

Lipophilicity	Enceleamycin A	Enceleamycin B	Enceleamycin C
Log <i>P</i> _{o/w} (iLOGP)	2.05	1.26	1.67
Log <i>P</i> _{o/w} (XLOGP3)	0.74	-1.06	0.46
Log <i>P</i> _{o/w} (WLOGP)	0.69	-1.15	0.53
Log <i>P</i> _{o/w} (MLOGP)	-0.73	-1.81	-1.21
Log <i>P</i> _{o/w} (SILICOS-IT)	1.41	0.03	1.76
Consensus Log <i>P</i> _{o/w}	0.83	-0.54	0.64

Table S9. Water solubility properties of Enceleamycins A-C by SwissADME

Water Solubility	Enceleamycin A	Enceleamycin B	Enceleamycin C
Log <i>S</i> (ESOL)	-2.54	-1.60	-2.30
Class	Soluble	Very soluble	Soluble
Log <i>S</i> (Ali)	-2.47	-1.45	-2.34
Class	Soluble	Very soluble	Soluble
Log <i>S</i> (SILICOS-IT)	-2.73	-1.57	-2.90
Class	Soluble	Soluble	Soluble

Table S10. Pharmacokinetics of Enceleamycins A-C by SwissADME

Pharmacokinetics	Enceleamycin A	Enceleamycin B	Enceleamycin C
GI absorption	High	Low	High
BBB permeant	No	No	No
P-gp substrate	Yes	Yes	No
CYP1A2 inhibitor	No	No	No
CYP2C19 inhibitor	No	No	No
CYP2C9 inhibitor	No	No	No
CYP2D6 inhibitor	No	No	No
CYP3A4 inhibitor	No	No	No
Log K_p (skin permeation)	-7.79 cm/s	-9.27 cm/s	-7.99 cm/s

Table S11. Druglikeness of Enceleamycins A-C by SwissADME

Druglikeness	Enceleamycin A	Enceleamycin B	Enceleamycin C
Lipinski	Yes; 0 violation	Yes; 0 violation	Yes; 0 violation
Veber	Yes	No; 1 violation: TPSA>140	Yes
Ghose	Yes	No; 1 violation: WLOGP<-0.4	Yes
Egan	Yes	No; 1 violation: TPSA>131.6	Yes
Muegge	Yes	Yes	Yes
Bioavailability Score	0.56	0.55	0.56

Table S12. Medicinal chemistry properties of Enceleamycins A-C by SwissADME

Medicinal Chemistry	Enceleamycin A	Enceleamycin B	Enceleamycin C
PAINS	1 alert: quinone_A	1 alert: keto_keto_gamma	1 alert: quinone_A
Brenk	0 alert	0 alert	1 alert: aldehyde
Leadlikeness	Yes	No; 1 violation: MW>350	Yes
Synthetic accessibility	4.84	4.76	4.64

Table S13. ADMET prediction profile of Enceleamycins A-C by the pkCSM webtool

Property	Model Name	Enceleamycin A	Enceleamycin B	Enceleamycin C	Unit
Absorption	Water solubility	-2.858	-3.088	-2.537	Numeric (log mol/L)
Absorption	Caco2 permeability	1.093	0.662	0.73	Numeric (log Papp in 10 ⁻⁶ cm/s)
Absorption	Intestinal absorption (human)	53.49	50.508	75.909	Numeric (% Absorbed)
Absorption	Skin Permeability	-2.719	-2.738	-3.148	Numeric (log Kp)
Absorption	P-glycoprotein substrate	Yes	Yes	Yes	Categorical (Yes/No)
Absorption	P-glycoprotein I inhibitor	No	No	No	Categorical (Yes/No)
Absorption	P-glycoprotein II inhibitor	No	No	No	Categorical (Yes/No)
Distribution	VDss (human)	-0.839	0.471	0.041	Numeric (log L/kg)
Distribution	Fraction unbound (human)	0.248	0.324	0.336	Numeric (Fu)
Distribution	BBB permeability	-0.423	-1.27	-0.146	Numeric (log BB)
Distribution	CNS permeability	-2.943	-3.581	-3.451	Numeric (log PS)
Metabolism	CYP2D6 substrate	Yes	No	No	Categorical (Yes/No)
Metabolism	CYP3A4 substrate	No	No	No	Categorical (Yes/No)
Metabolism	CYP1A2 inhibitor	No	No	No	Categorical (Yes/No)
Metabolism	CYP2C19 inhibitor	No	No	No	Categorical (Yes/No)
Metabolism	CYP2C9 inhibitor	No	No	No	Categorical (Yes/No)
Metabolism	CYP2D6 inhibitor	No	No	No	Categorical (Yes/No)
Metabolism	CYP3A4 inhibitor	No	No	No	Categorical (Yes/No)
Excretion	Total Clearance	1.231	0.724	-0.13	Numeric (log ml/min/kg)
Excretion	Renal OCT2 substrate	No	No	No	Categorical (Yes/No)
Toxicity	AMES toxicity	No	No	No	Categorical (Yes/No)
Toxicity	Max. tolerated dose (human)	0.689	0.217	-0.056	Numeric (log mg/kg/day)
Toxicity	hERG I inhibitor	No	No	No	Categorical (Yes/No)
Toxicity	hERG II inhibitor	No	No	No	Categorical (Yes/No)
Toxicity	Oral Rat Acute Toxicity (LD50)	2.478	3.364	2.738	Numeric (mol/kg)
Toxicity	Oral Rat Chronic Toxicity (LOAEL)	1.932	3.274	1.819	Numeric (log mg/kg_bw/day)
Toxicity	Hepatotoxicity	No	No	No	Categorical (Yes/No)
Toxicity	Skin Sensitisation	No	No	No	Categorical (Yes/No)
Toxicity	T.Pyriformis toxicity	0.205	0.285	0.3	Numeric (log ug/L)
Toxicity	Minnow toxicity	1.97	3.596	2.005	Numeric (log mM)

Reference:

1. A. Khan, M. S. Said, B. R. Borade, R. Gonnade, V. Barvkar, R. Kontham and S. G. Dastager, *J. Nat. Prods.*, 2022, 85, 1267-1273.
2. V. Vichai and K. Kirtikara. *Nat. Protoc.*, 2006, **1** , 1112–1116.
3. J. Kode, J. Kovvuri, B. Nagaraju, S. Jadhav, M. Barkume, S. Sen, N. K. Kasinathan, P. Chaudhari, B. S. Mohanty, J. Gour, D. K. Sigalapalli, C. G. Kumar, T. Pradhan, M. Banerjee and A. Kamal. *Bioorg. Chem.*, 2020, **105** , 104447.